

Electrostatic modulation of hnRNPA1 low-complexity domain liquid–liquid phase separation and aggregation

Phoebe S. Tsoi | My Diem Quan | Kyoung-Jae Choi | Khoa M. Dao |
Josephine C. Ferreon | Allan Chris M. Ferreon 

Department of Pharmacology and
Chemical Biology, Baylor College of
Medicine, Houston, Texas

Correspondence

Josephine C. Ferreon and Allan Chris
M. Ferreon, Department of Pharmacology
and Chemical Biology, Baylor College of
Medicine, Houston, TX 77030 USA.
Email: josephine.ferreon@bcm.edu and
allan.ferreon@bcm.edu

Funding information

National Institute of General Medical
Sciences, Grant/Award Number: R01
GM122763; National Institute of
Neurological Disorders and Stroke, Grant/
Award Numbers: F31 NS103380, R01
NS105874, R21 NS107792, R21 NS109678

Abstract

Membrane-less organelles and RNP granules are enriched in RNA and RNA-binding proteins containing disordered regions. Heterogeneous nuclear ribonucleoprotein A1 (hnRNPA1), a key regulating protein in RNA metabolism, localizes to cytoplasmic RNP granules including stress granules. Dysfunctional nuclear-cytoplasmic transport and dynamic phase separation of hnRNPA1 leads to abnormal amyloid aggregation and neurodegeneration. The intrinsically disordered C-terminal domain (CTD) of hnRNPA1 mediates both dynamic liquid–liquid phase separation (LLPS) and aggregation. While cellular phase separation drives the formation of membrane-less organelles, aggregation within phase-separated compartments has been linked to neurodegenerative diseases. To understand some of the underlying mechanisms behind protein phase separation and LLPS-mediated aggregation, we studied LLPS of hnRNPA1 CTD in conditions that probe protein electrostatics, modulated specifically by varying pH conditions, and protein, salt and RNA concentrations. In the conditions investigated, we observed LLPS to be favored in acidic conditions, and by high protein, salt and RNA concentrations. We also observed that conditions that favor LLPS also enhance protein aggregation and fibrillation, which suggests an aggregation pathway that is LLPS-mediated. The results reported here also suggest that LLPS can play a direct role in facilitating protein aggregation, and that changes in cellular environment that affect protein electrostatics can contribute to the pathological aggregation exhibited in neurodegeneration.

KEYWORDS

ALS, hnRNPA1, intrinsically disordered protein, LLPS, neurodegenerative diseases, protein aggregation

Abbreviations: AD, Alzheimer's disease; ALS, amyotrophic lateral sclerosis; CTD, C-terminal domain; FTD, frontotemporal dementia; hnRNPA1, heterogeneous nuclear ribonucleoprotein A1; IDP, intrinsically disordered protein; LCD, low-complexity domain; LLPS, liquid–liquid phase separation; MLOs, membrane-less organelles; RBD/P, RNA binding domain/protein; SGs, stress granules; ThT, Thioflavin T.

1 | INTRODUCTION

Recent studies suggest that cells organize many biochemical processes in membrane-less compartments that exhibit liquid-like properties.^{1,2} These membrane-less organelles (MLOs) are hubs of proteins, RNA, or DNA

molecules that condense at specific subcellular loci to fulfill defined biological functions.^{1,3} Given that constituent macromolecules can be rapidly exchanged between the loci and cytoplasm, researchers have proposed that MLOs arise through a process of liquid–liquid phase separation (LLPS).⁴ Many MLOs, such as stress granules (SGs) and P-bodies, dynamically assemble and disassemble in response to cellular stress and other stimuli.^{5,6} Extensive studies have identified that many RNA-binding proteins, for example, hnRNPA1 and TDP-43, largely contribute to this conditional cellular compartmentalization.^{7,8} Although the molecular details underlying LLPS in cells are largely obscure, several reports indicate that constituent proteins harboring low-complexity domains (LCDs) can mediate this process through weak multivalent interactions.^{3,9,10} Interestingly, proteins containing LCDs are also prone to amyloid aggregation, which is closely associated to the pathogenesis of a myriad of neurodegenerative diseases including amyotrophic lateral sclerosis (ALS), Alzheimer's disease (AD), and frontotemporal dementia (FTD).^{7,8,11} Unraveling the driving factors of LLPS

and amyloid fibril formation is imperative to understanding the pathophysiology of neurodegeneration.

The structure of hnRNPA1, a prominent member of the heterogeneous nuclear ribonucleoproteins (hnRNP) family, consists of two N-terminal folded RNA-binding domains (RBDs) and an intrinsically disordered low-complexity C-terminal domain (CTD; Figure 1a).¹² hnRNPA1 and other members in its family participate in many aspects of RNA metabolism, including mobilizing mRNAs in SG formation.^{13,14} SGs are MLOs that form in response to cellular and environmental stressors, and transiently store translationally stalled mRNAs until stress is resolved.⁶ Because SGs dynamically assemble and disassemble, it has been suggested that SGs originate from LLPS.^{1,6,15} Various forms of stress are known to cause SG formation, including oxidative, osmotic, and acid stress.¹⁶ Prolonged existence of SGs or increased SG formation accelerates the pathophysiology of neurodegenerative protein aggregation.¹⁷ Given its association with SGs, hnRNPA1 mislocalization and dysregulation have been implicated in ALS, AD, and FTD.^{8,11,18–20} Despite hnRNPA1's neuropathological significance,

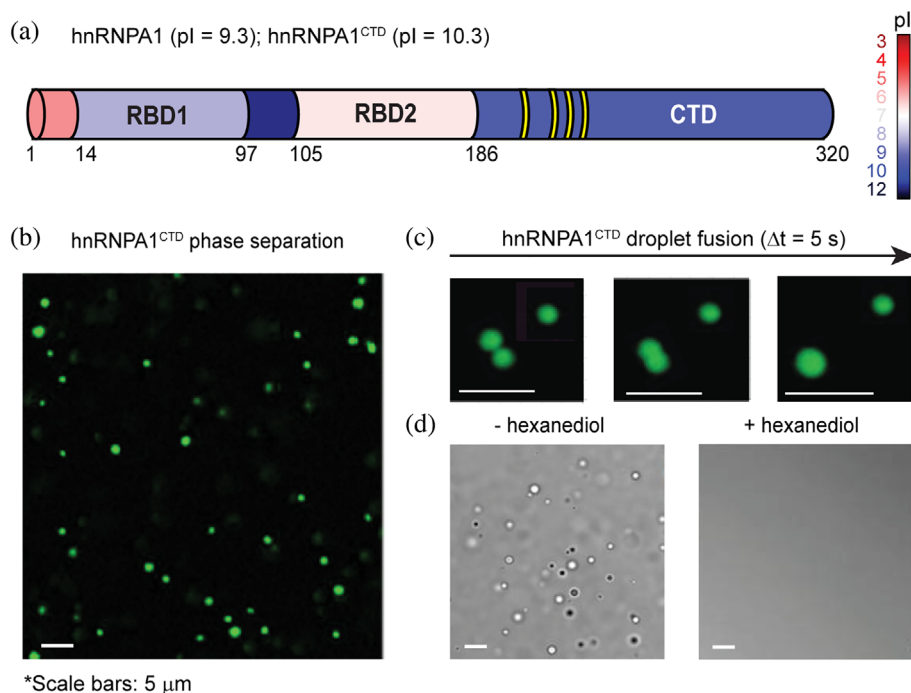


FIGURE 1 The low-complexity domain of the heterogeneous nuclear ribonucleoprotein hnRNPA1 reversibly phase separates into liquid-like droplets. (a) Heterogeneous nuclear ribonucleoprotein A1 (hnRNPA1) domain organization. Protein segments are color-coded on the basis of their isoelectric point (pI). RGG recognition motifs in the C-terminal domain (CTD) are highlighted in yellow. (b) Fluorescence microscopy image of hnRNPA1^{CTD} liquid–liquid phase separation (LLPS) in the absence of molecular crowding agent. Liquid droplets are enriched in Alexa Fluor 488-labeled hnRNPA1^{CTD} (1:200 molar ratio of labeled to unlabeled hnRNPA1^{CTD}). (c) Temporal fusion of Alexa Fluor 488-labeled hnRNPA1^{CTD} droplets. Protein droplets merge over time, demonstrating liquid-like nature. (d) Differential interference contrast (DIC) microscopy images of hnRNPA1^{CTD} solution before and after the addition of 5% (vol/vol) 1,6-hexanediol, showing droplet formation reversibility and liquid-like property. Experimental solution conditions: 20 μ M hnRNPA1^{CTD} in 300 mM NaCl; 10 mM sodium acetate, 10 mM sodium phosphate, 10 mM glycine ($\alpha\beta$ buffer); pH 7.0

mechanisms and driving forces of its LLPS and pathologic aggregation remain largely unknown. In this paper, we investigate the effects of pH on salt- and RNA-dependent hnRNPA1^{CTD} phase separation. We demonstrate that the CTD undergoes electrostatic-mediated LLPS and that pH modulates phase separation thresholds, and aggregation propensity and kinetics of hnRNPA1^{CTD} droplets. Characterizing these electrostatic interactions will elucidate the evolution of a protective cellular mechanism into a neurodegenerative disease-causing phenomenon.

2 | RESULTS

2.1 | The hnRNPA1 low-complexity domain undergoes liquid–liquid phase separation

To gain insight into the forces that drive the LLPS of low-complexity regions of intrinsically disordered proteins (IDPs), we use as a model the C-terminal domain (CTD) of the heterogeneous nuclear ribonucleoprotein hnRNPA1 (hnRNPA1^{CTD}), expressed and purified initially as a fusion protein with solubility-enhancing His-mCherry tag (His-mCherry-hnRNPA1^{CTD}). hnRNPA1, a highly alkaline RNA-binding protein (RBP; pI>10), consists of two structured N-terminal RNA-binding domains (RBD1 and RBD2) and an intrinsically disordered CTD that harbors four RGG recognition motifs known to associate with ribonucleic acids and modulate phase separation^{21,22} (Figure 1a). Untagged hnRNPA1^{CTD} was fluorescently labeled by N-terminal conjugation to Alexa Fluor 488 dye and observed to separate into distinct liquid phases (Figure 1b), inducible by increasing salt concentration without the aid of a molecular crowding agent. These protein droplets can undergo rapid fusion, reflecting liquid properties (Figure 1c). Addition of 5% (vol/vol) 1,6-hexanediol, a compound that disrupts aromatic interactions known to contribute to LLPS,²³ reverses droplet formation (Figure 1d).

2.2 | hnRNPA1^{CTD} LLPS is modulated by pH, and protein, salt and RNA concentrations

SGs are enriched in RBPs and translationally stalled mRNAs.²⁴ These granules form in response to stressors that perturb the cellular microenvironment, including acid stress.¹⁶ Recent studies have demonstrated that hnRNPA1 phase separates and is recruited to SGs.^{12,15} To investigate the electrostatic forces that promote

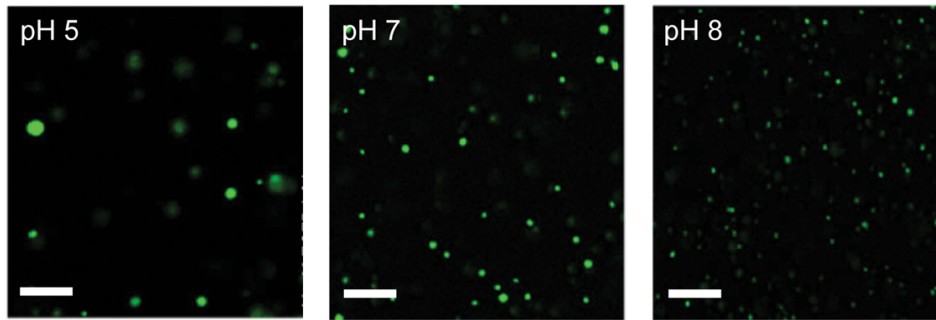
hnRNPA1^{CTD} phase separation, we varied the concentrations of protein, NaCl and RNA in pH 4, 5, 6, 7 and 8 conditions and observed hnRNPA1^{CTD} droplet formation (Figure 2a–e). We observed that the propensity of hnRNPA1^{CTD} to undergo LLPS was strongly pH-dependent (Figure 2a,d,e). At constant salt concentration and incubation time, acidic pH promoted formation of larger hnRNPA1^{CTD} droplets while neutral and basic conditions induced smaller liquid droplets (Figure 2a). We detected turbidity at the spectroscopically inactive wavelength of 600 nm (Figure 2b) and measured droplet sizes (Figure 2c), and observed both parameters to inversely correlate with pH, that is, light scattering and droplet dimensions decrease as pH increases.

We summarized our findings for both the salt-dependent and the RNA-dependent LLPS of hnRNPA1^{CTD} using two sets of phase diagrams (Figure 2d,e). Higher NaCl concentrations consistently decreased the protein concentration thresholds for LLPS (Figure 2d), which was further minimized at more acidic pH conditions. Conversely, as the pH approaches physiological and basic conditions, the protein concentration thresholds increased, thereby requiring higher salt and protein concentrations to induce droplet formation. Similar yet more pronounced trends were observed in the RNA-dependent hnRNPA1^{CTD} phase separation (Figure 2e). At physiological pH, RNA promoted LLPS even at approximately 3 μ M hnRNPA1^{CTD} whereas salt minimally induced phase separation even with 12 μ M hnRNPA1^{CTD}.

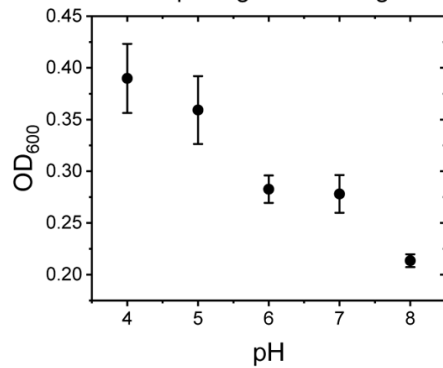
2.3 | hnRNPA1^{CTD} LLPS-mediated aggregation is modulated by pH conditions, and salt and RNA concentrations

While examining hnRNPA1^{CTD} LLPS properties, we observed that reversible droplet assembly was accompanied by the formation of protein aggregates within a few hours in most of our experimental conditions. To investigate the role of phase separation in driving protein aggregation and fibrillation, we employed a Thioflavin T (ThT) fluorescence assay to test the correlation between hnRNPA1^{CTD} LLPS and aggregation, varying pH conditions, and salt and RNA concentrations (Figure 3a–d).

Incubation of hnRNPA1^{CTD} droplets in both LLPS-unfavorable and LLPS-favorable salt conditions (10–50 mM and 100–1,000 mM, respectively; Figure 3a) with ThT dye resulted in the formation of ThT-positive aggregates. We observed that LLPS-inducing conditions resulted in the rapid formation of aggregates, usually within 2–6 hr, and exhibited high ThT fluorescence intensity endpoints (Figure 3a). In contrast, non-LLPS-inducing conditions resulted to slower aggregation

(a) hnRNPA1^{CTD} pH-dependent phase separation

(b) Droplet light scattering



(c) Droplet dimension

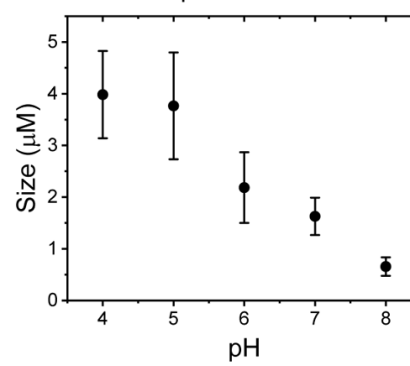
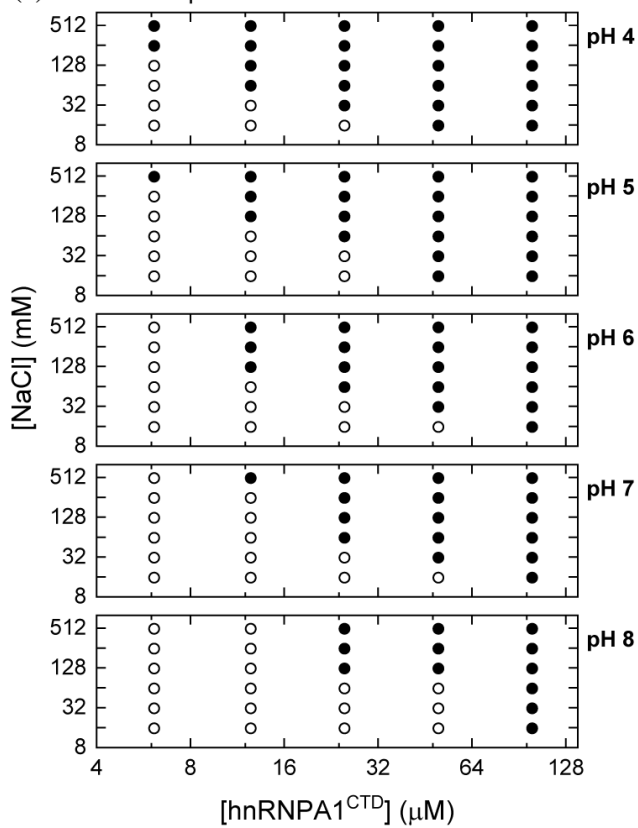
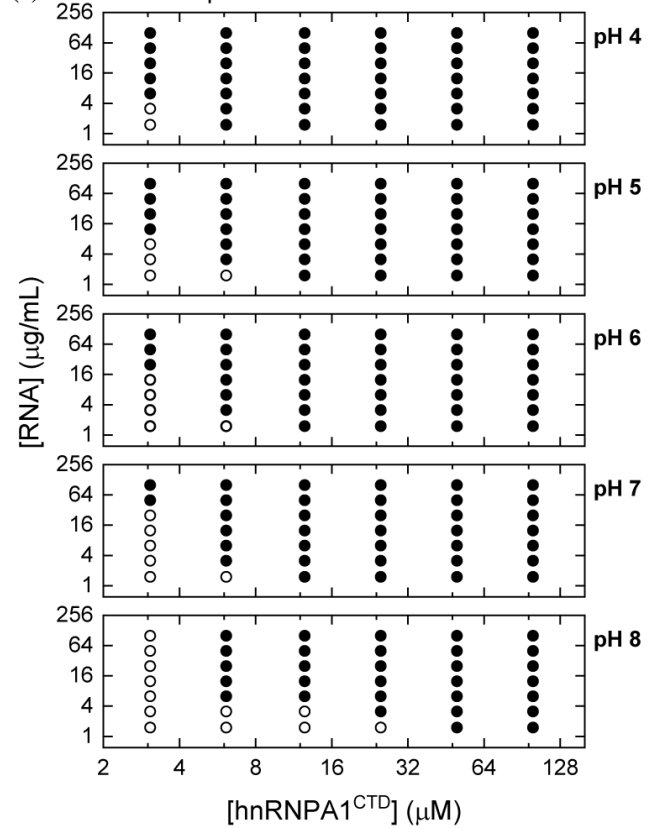
(d) Salt-dependence of hnRNPA1^{CTD} LLPS(e) RNA-dependence of hnRNPA1^{CTD} LLPS

FIGURE 2 Legend on next page.

kinetics and lower ThT fluorescence intensity endpoints (Figure 3a). Furthermore, pH also affected the formation rate of aggregates, with more acidic pH conditions generally demonstrating faster aggregation initiation (with minimal nucleation or lag phase) and reaching the maximal ThT fluorescence intensity endpoints earlier as compared to the neutral and alkaline counterparts.

Similarly, hnRNPA1^{CTD} aggregation experiments were also performed at varying RNA concentrations (non-LLPS condition: 1 $\mu\text{g/ml}$; LLPS-inducing conditions: 10–1,000 $\mu\text{g/ml}$), and parallel results were observed (Figure 3c). Notably, the final fluorescence intensity maxima were generally higher for RNA-dependent LLPS-mediated aggregates as compared to those in the salt-dependent conditions. Strikingly, ThT-positive aggregates formed in the presence of minimal RNA (1 $\mu\text{g/ml}$) at pH 6, 7 and 8, with the fastest appearance occurring after 3 hr in pH 6.

The time elapsed to attain half-maximum ThT fluorescence signal ($t_{1/2}$) was determined for each experimental condition and plotted as exponential decays to more clearly illustrate the observed trends (Figure 3b,d). In general, conditions of higher NaCl or RNA concentrations and lower pH displayed shorter $t_{1/2}$ whereas conditions of lower NaCl or RNA concentrations and higher pH showed longer $t_{1/2}$. Furthermore, the trend is more pronounced in salt-dependent hnRNPA1^{CTD} aggregation. Overall, these results show that electrostatic forces modulate the aggregation propensity of hnRNPA1^{CTD}, and that acidic pH conditions as well as high protein and salt/polyelectrolyte/multivalent ligand concentrations favor hnRNPA1^{CTD} aggregation.

3 | DISCUSSION

Studies have shown that many aggregation-prone proteins involved in neurodegenerative diseases also undergo LLPS.^{15,25–27} Although aggregation does not necessarily proceed via LLPS, with protein aggregation/fibrillation and phase separation being two independent processes,²⁶ highly enriched phase-separated proteins

usually exhibit greater tendency to aggregate compared to more dilute homogeneous protein solutions. Here, our work demonstrates that hnRNPA1^{CTD} is able to assemble into protein-rich droplets via LLPS (Figure 1), and such *in vitro* phase separation is tunable by variables that modulate electrostatic forces. Specifically, higher salt and RNA concentrations and acidic pH conditions reduce the hnRNPA1^{CTD} protein concentration threshold required for LLPS. We further observed temporal formation of ThT-positive aggregates in conditions favorable to hnRNPA1^{CTD} droplet formation (Figure 3). The structural flexibility and conformational freedom exhibited by proteins/domains with low sequence complexity, as is the case for intrinsically disordered proteins – IDPs and proteins with significant intrinsically disordered regions – IDRs, combined with the inherent capacity for multivalent interactions and propensity for nonspecific interactions are characteristics that can drive LLPS, the formation of mesh-like networks of biomolecules. Separation from the bulk phase into liquid droplets is the result of a dynamic interplay between energetically favorable and unfavorable interactions within the network versus that in the surrounding solution. Potential bias for aggregation afforded by the liquid droplet environment (e.g., changes in local pH and/or salt/polyelectrolyte/multivalent ligand concentrations) and the resultant increased protein concentration pose significant risks *in vivo* as with SGs. Hubs of promiscuous weak-interacting proteins prolonged by dysfunctional clearance can eventually lead to cytotoxic aggregates identified in neurodegenerative diseases.²⁸

In the solution conditions we tested, we find that hnRNPA1^{CTD} readily phase separates, aided only by salt and/or RNA (a polyelectrolyte and weakly-interacting multivalent ligand), in the absence of non-physiological molecular crowding agents that have the potential to complicate experiments involving multiple variables. Here, we show that pH plays a regulatory role in hnRNPA1^{CTD} LLPS as lower concentrations of salt or nucleic acids are required with increasingly acidic conditions. Provided that varying pH conditions and concentrations of salt and RNA controls the hnRNPA1^{CTD}

FIGURE 2 Modulation of heterogeneous nuclear ribonucleoprotein A1 C-terminal domain (hnRNPA1^{CTD}) liquid–liquid phase separation (LLPS) by varying pH, and protein, salt and RNA concentrations. (a) Representative fluorescence microscopy images of 20 μM Alexa Fluor 488-labeled hnRNPA1^{CTD} with 1 mg/ml RNA at pH 5, 7 and 8. While phase separation occurred in all pH conditions, LLPS is favored at lower pH. (b) LLPS monitored by optical density (OD₆₀₀) measured at 600 nm after 5 min of incubation. Measured optical density increased with increasing solution acidity. Error bars represent measurement standard deviations. Conditions: 20 μM Alexa Fluor 488-labeled hnRNPA1^{CTD}, 1 mg/ml RNA, 10 mM NaCl in $\alpha\beta\gamma$ buffer, pH 4–8 ($n = 3$). (c) Droplet dimensions at different pH conditions after 5 min of incubation. Droplet size increased with increasing solution acidity. Same experimental solution conditions as (b) ($n = 100$). (d) and (e) Phase diagrams depicting the salt concentration-dependence and RNA concentration-dependence of hnRNPA1^{CTD} LLPS from pH 4 to 8. Open circles (○) and closed circles (●) indicate the absence and presence of phase separation, respectively

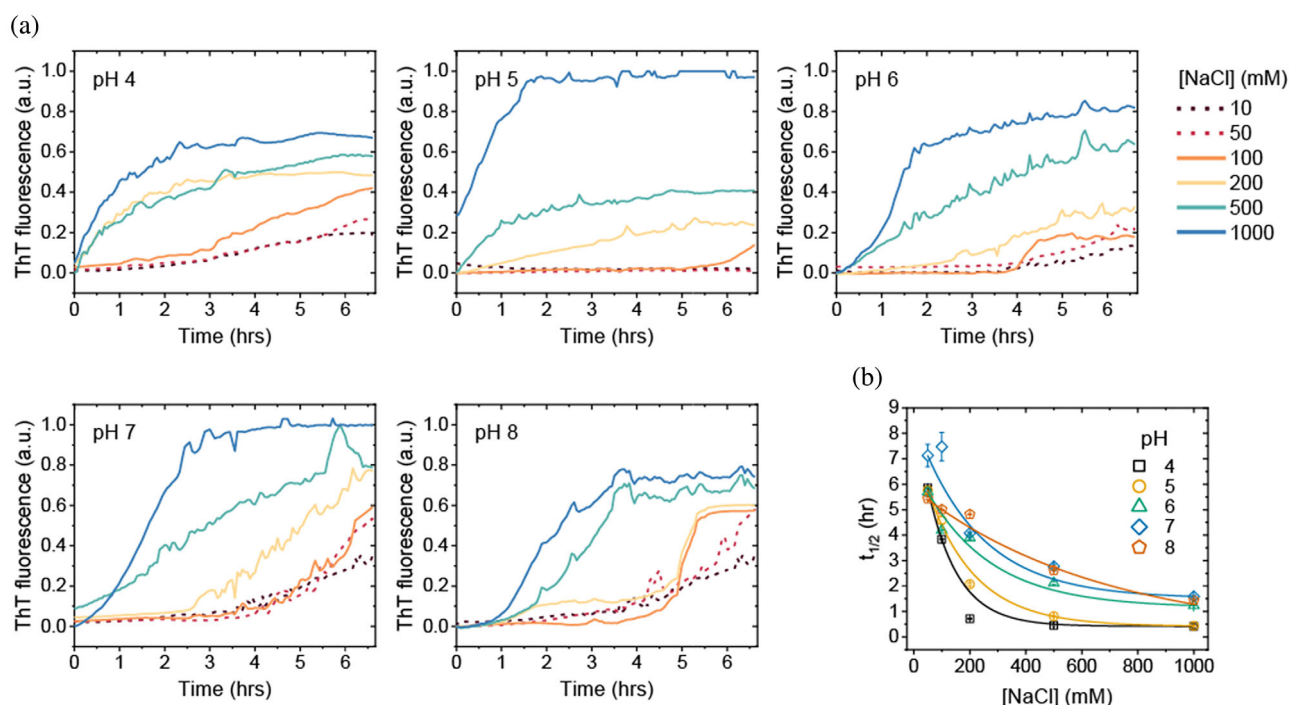
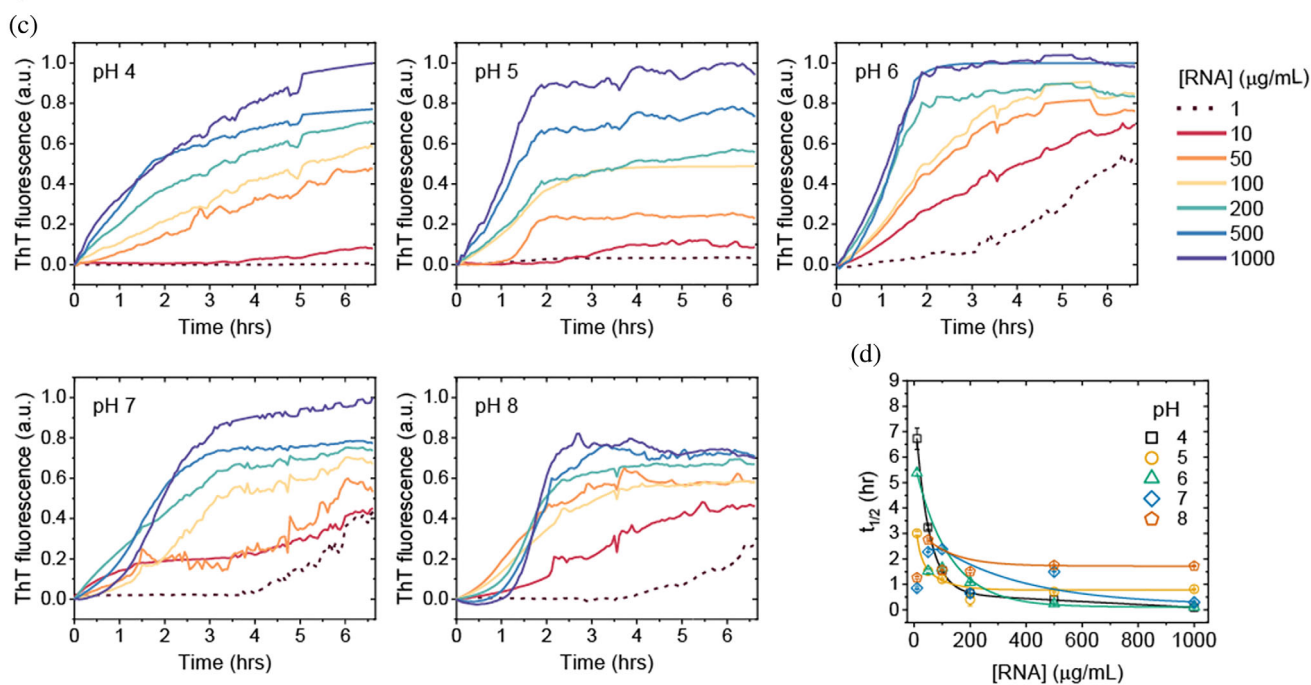
Salt-dependence of hnRNPA1^{CTD} aggregation vs. pHRNA-dependence of hnRNPA1^{CTD} aggregation vs. pH

FIGURE 3 Solution pH, and salt and RNA concentrations tune heterogeneous nuclear ribonucleoprotein A1 C-terminal domain (hnRNPA1^{CTD}) aggregation. hnRNPA1^{CTD} aggregation kinetics at varying salt (a,b), RNA (c,d), and pH (a-d) conditions monitored by Thioflavin T (ThT) fluorescence over 6 hr. Solid and dashed lines indicate aggregation proceeding in LLPS-favorable or unfavorable conditions, respectively. Time elapsed to attain half-maximum ThT fluorescence signal ($t_{1/2}$) plotted as functions of NaCl and RNA concentrations (b, d). $t_{1/2}$ values for the aggregation reactions were determined using the Boltzmann equation and fitted as exponential decays for visual guide. Conditions: 20 μ M hnRNPA1^{CTD}, 3 μ M ThT, α β buffer at pH 4–8 ($n = 3$)

concentration threshold for LLPS, our data also suggest that electrostatic forces are a regulatory element of phase separation. Given that pH modulates a protein's protonation state, it has been shown that folded, stable proteins become more insoluble in conditions nearing their isoelectric point as the proteins' gradual net loss of charges reduces the number of hydrogen bonding with surrounding water molecules.²⁹ In the case of hnRNPA1^{CTD}, in pH conditions approaching its pI of 10.3, LLPS propensity as well as droplet size decreased (Figure 2). In contrast, the presence of salt and RNA greatly favors the phase separation of hnRNPA1^{CTD} across all pH conditions. hnRNPA1^{CTD} alone did not phase separate in the range of protein concentrations in which our experiments were conducted. Interaction with ions in solution allowed hnRNPA1^{CTD} to overcome the protein concentration minima and undergo LLPS. Our results with RNA, which can also be visualized as a large polyelectrolyte, suggest that some electrostatic interaction is required between the alkaline hnRNPA1^{CTD} and anions for LLPS to occur. This electrostatic interaction is more favorable in more acidic pH conditions as the hnRNPA1^{CTD} gradually gains a more positive/less negative net charge. Furthermore, RNA may act as a multivalent weakly-interacting ligand recognized by hnRNPA1^{CTD} RGG motifs (Figure 1a), providing nonspecific interactions to recruit additional proteins to form liquid droplets.

While we observed that increasing acidity encourages hnRNPA1^{CTD} LLPS and aggregation, such characteristics cannot be generally applied across all systems that undergo phase separation. Some intrinsically disordered proteins such as α -synuclein have exhibited similar acidic pH-dependent solubility/aggregation trends³⁰ while others like TDP-43 have been shown to exhibit the opposite trend.³¹ Mompean et al. presents a case that repulsive electrostatic forces govern TDP-43^{CTD} LLPS and that lower pH adds to the protein's net charge, which subsequently disfavors phase separation.³² Comparing the charge of TDP-43^{CTD} and hnRNPA1^{CTD} reveals that TDP-43^{CTD} is more positively charged in acidic pH environments (reported +13.2³¹ for TDP-43^{CTD} vs +11 for hnRNPA1^{CTD} at pH 4, calculated at <http://protcalc.sourceforge.net/>). hnRNPA1^{CTD} is more positively charged at acidic pH compared to higher pH, and our data suggest that some positive charges on hnRNPA1^{CTD} favor LLPS, potentially via ionic interactions with salts and polyanions, and allow for tuning via electrostatic forces. We acknowledge that other solution conditions (e.g., the presence of osmolytes) as well as inter- and intramolecular forces beyond electrostatic interactions also drive phase separation and should not be disregarded.^{33–35} Overall, LLPS is a complex phenomenon whose mechanisms and regulation deserve further research.

Our data not only demonstrate electrostatic interactions tinkering with LLPS but also a strong accelerating effect of salt and RNA on aggregation kinetics (Figure 3). Greater salt and RNA concentrations generally increased hnRNPA1^{CTD} aggregation across all pH conditions. Specifically, more acidic pH conditions exhibited shorter lag times for both salt- and RNA-dependent protein aggregation. Conversely, alkaline conditions showed longer lag phases and discouraged aggregation. Interestingly, at constant pH, the concentrations of salt and RNAs at which hnRNPA1^{CTD} droplets formed had shorter lag times (smaller $t_{1/2}$ values) compared to conditions where LLPS was not observed, suggesting that the same electrostatic forces that drive phase separation also play a role in hnRNPA1^{CTD} aggregation. Such accelerated aggregation may be related to the formation of amyloid-like structures common to many neurodegeneration-associated IDPs that form ThT-positive fibrillary aggregates. A recently discovered amyloid folding core capable of assembling reversible fibrils is present within hnRNPA1^{CTD}, further suggesting that the aggregation in the protein-rich droplet phase may be amyloid.³⁶ Despite these observations, LLPS and aggregation are not always linked. We recently demonstrated the decoupling of LLPS and fibrillation via the chemical chaperone/osmolyte trimethylamine N-oxide (TMAO) using TDP-43 as a model system, which suggests that the phase separation induced by similar compounds may protect against amyloid formation.²⁶ Other studies on hnRNPA1 have also shown that LLPS and aggregation are independent processes.⁸ The formation of ThT-positive hnRNPA1^{CTD} aggregates in LLPS-unfavorable conditions further supports phase separation and aggregation as independent processes. Across all experimental conditions, we observed greater final ThT fluorescence signals in LLPS-favorable vs LLPS-unfavorable conditions (Figure 3a,c) during the observation window, suggesting the existence of LLPS-independent aggregation pathway/s. Such consistent trend warrants future studies to understand LLPS-mediated and LLPS-independent aggregation pathways for neurodegenerative disease-associated IDPs.

Our results examine the impact of pH on salt- and RNA-dependent LLPS and aggregation of hnRNPA1^{CTD} (Figure 4). In summary, we showed hnRNPA1^{CTD} LLPS to be modulated by electrostatic interactions, particularly by using pH, and salt and RNA concentrations as variables. Detection of ThT-positive aggregates in both LLPS- and non-LLPS-inducing conditions suggests the plausibility of two aggregation pathways: LLPS-mediated and LLPS-independent, which can also be affected by LLPS-modulating factors. These *in vitro* observations do not completely reflect the mechanisms of recruitment or aggregation of SG-related proteins; however, self-

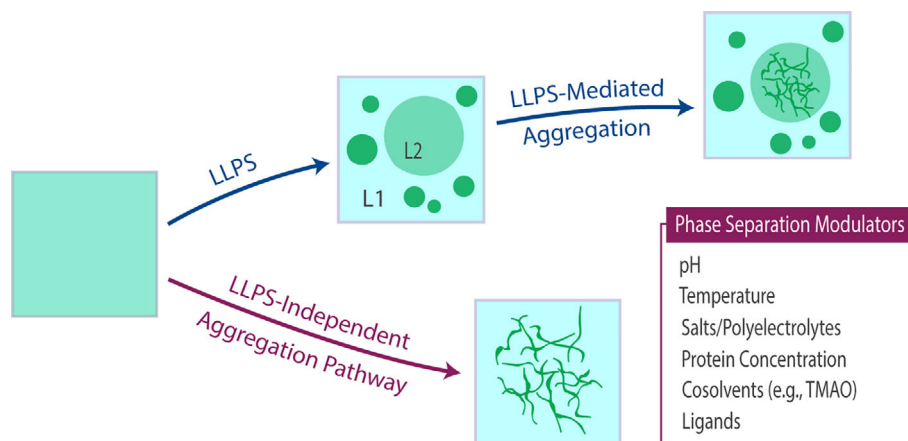


FIGURE 4 Electrostatic modulation of liquid–liquid phase separation (LLPS)-mediated (*indirect*) and LLPS-independent (*direct*) protein aggregation pathways. Although enhancement of LLPS is not necessarily linked with increased protein aggregation propensity, the same physicochemical properties that modulate phase separation can also affect protein aggregation, which can manifest in the initial non-phase separated solution (i.e., LLPS-independent protein aggregation) and/or occur in either of the two resultant liquid phases (i.e., LLPS-mediated protein aggregation; L1 and L2). Enhancement or inhibition of protein aggregation via LLPS depends on the specific phase solution microenvironments

association mechanisms similar to LLPS-mediated fibrillation may exist *in vivo*. The hypothesis that LLPS may mediate formation of pathological hnRNPA1 aggregates in neurodegenerative diseases is supported by recent observations that hnRNPA1 aggregates appear to localize to stress granules in ALS, FTD, and AD.^{8,11} Consistent with these findings, our data suggest that LLPS may play a direct role in hnRNPA1^{CTD} aggregation, likely by providing an environment not only of increased local protein concentration but also of other solution components that simultaneously enhance LLPS and protein self-interaction.

4 | MATERIALS AND METHODS

4.1 | Protein expression, purification, and labeling

His6-mCherry-tev cleavage site-hnRNPA1^{CTD} was expressed in DE3 *Escherichia coli* Rosetta cells (Novagen, Merck KGaA, Darmstadt, Germany) in terrific broth (TB) medium. Cells were grown at 37°C in the presence of kanamycin and chloramphenicol until the optical density at 600 nm (OD₆₀₀) reaches 0.8–1.0, then induced with 1 mM isopropyl β-d-1-thiogalactopyranoside and grown overnight at 18°C. Cells were resuspended in 500 mM NaCl, 10 mM imidazole, 50 mM Tris, pH 8 with a protease inhibitor cocktail (GenDEPOT, Katy, TX) before lysis using a cell homogenizer (Avestin, Ottawa, Canada). The lysate was centrifuged and supernatant was loaded onto a

gravity HisPur column (Thermo Fisher Scientific, Waltham, MA), washed with the lysis buffer and eluted with 500 mM NaCl, 300 mM imidazole, 50 mM Tris, pH 8. The protein solution was dialyzed overnight with lysis buffer and 1:50 mass ratio of TEV protease for cleavage of the His-mCherry tag. The tag was removed using cobalt column. The flow-through was concentrated and further purified by reverse-phase HPLC using a C3 column (Agilent, Santa Clara, CA). The protein solution was dialyzed against water and stored at –80°C until later use. Proteins were labeled using NHS ester chemistry with Alexa Fluor 488 dye (Thermo Fisher Scientific) at a 1:10 protein: dye ratio, incubating for 2 hr at room temperature. Labeled protein was purified using HPLC.

4.2 | hnRNPA1^{CTD} LLPS experiments

Purified hnRNPA1^{CTD} liquid–liquid phase separation (LLPS) experiments were performed using variable protein (0–100 μM), salt (0–1 M NaCl), and RNA (0–1,000 μg/ml) concentrations in αβγ buffer (10 mM sodium acetate, 10 mM NaH₂PO₄, 10 mM glycine) in pH conditions ranging from pH 4–8. 10–20-μl drops were pipetted onto 35 mm glass bottom dishes (ibidi, Martinsried, Germany) and monitored for droplet formation (with incubation time of 5 min) using EVOS FL (ThermoFisher Scientific) optical and fluorescence microscopy. Turbidity was measured using Nanodrop2000 (ThermoFisher Scientific), and droplet sizes were determined using ImageJ³⁷ particle selection analysis.

4.3 | ThT fluorescence assay

hnRNPA1^{CTD} aggregation was detected by monitoring changes in thioflavin T (ThT) fluorescence using a Tecan Spark plate reader, employing 440 nm excitation and 480 nm emission wavelengths. Protein aggregation reactions were conducted using 20 μ M hnRNPA1^{CTD}, 3 μ M ThT (GenDepot), 10–1,000 mM NaCl conditions or 1–1,000 μ g/ml torula yeast RNA (Sigma Aldrich, St. Louis, MO), 10 mM α β buffer in pH conditions ranging from pH 4–8. Aggregation kinetics were monitored for over 6 hr.

Half-maximum ThT fluorescence was determined using Boltzmann equation, a function used to describe sigmoidal patterns, as given by:

$$Y = A_2 + \frac{A_1 - A_2}{1 + e^{(x-x_0)/dx}}$$

where A_1 is the minimal baseline and A_2 is the maximal baseline, x_0 is the time at which the change in signal is at 50% ($t_{1/2}$), and dx is the time constant.

ACKNOWLEDGEMENTS

This research was supported by a National Institute of Neurological Disorders and Stroke (NINDS), National Institutes of Health grant R21 NS107792 to Allan Chris M. Ferreon. Additional funding provided by R01 NS105874 and R21 NS109678 to Allan Chris M. Ferreon; R01 GM122763 to Josephine C. Ferreon; and, F31 NS103380 to Phoebe S. Tsoi.

CONFLICT OF INTEREST

The authors declare no conflicts of interest.

AUTHOR CONTRIBUTIONS

Phoebe S. Tsoi: Conceptualization; data curation; formal analysis; funding acquisition; investigation; methodology; validation; visualization; writing-original draft; writing-review & editing. **My Quan:** Data curation; formal analysis; visualization; writing-original draft; writing-review & editing. **Kyoung-Jae Choi:** Methodology; writing-review & editing. **Khoa M. Dao:** Methodology; writing-review & editing. **Josephine C. Ferreon:** Conceptualization; funding acquisition; methodology; project administration; resources; supervision; writing-review & editing. **Allan Chris M. Ferreon:** Conceptualization; data curation; formal analysis; funding acquisition; project administration; resources; supervision; visualization; writing-original draft; writing-review & editing.

ORCID

Allan Chris M. Ferreon  <https://orcid.org/0000-0002-8538-1732>

REFERENCES

1. Brangwynne CP, Eckmann CR, Courson DS, et al. Germline P granules are liquid droplets that localize by controlled dissolution/condensation. *Science*. 2009;324:1729–1732.
2. Brangwynne CP, Mitchison TJ, Hyman AA. Active liquid-like behavior of nucleoli determines their size and shape in *Xenopus laevis* oocytes. *Proc Natl Acad Sci U S A*. 2011;108:4334–4339.
3. Nott TJ, Petsalaki E, Farber P, et al. Phase transition of a disordered nuage protein generates environmentally responsive membraneless organelles. *Mol Cell*. 2015;57:936–947.
4. Hyman AA, Weber CA, Julicher F. Liquid-liquid phase separation in biology. *Annu Rev Cell Dev Biol*. 2014;30:39–58.
5. Anderson P, Kedersha N. RNA granules. *J Cell Biol*. 2006;172:803–808.
6. Buchan JR, Parker R. Eukaryotic stress granules: The ins and outs of translation. *Mol Cell*. 2009;36:932–941.
7. Sreedharan J, Blair IP, Tripathi VB, et al. TDP-43 mutations in familial and sporadic amyotrophic lateral sclerosis. *Science*. 2008;319:1668–1672.
8. Kim HJ, Kim NC, Wang YD, et al. Mutations in prion-like domains in hnRNPA2B1 and hnRNPA1 cause multisystem proteinopathy and ALS. *Nature*. 2013;495:467–473.
9. Elbaum-Garfinkle S, Kim Y, Szczepaniak K, et al. The disordered P granule protein LAF-1 drives phase separation into droplets with tunable viscosity and dynamics. *Proc Natl Acad Sci U S A*. 2015;112:7189–7194.
10. Martin EW, Mittag T. Relationship of sequence and phase separation in protein low-complexity regions. *Biochemistry*. 2018;57:2478–2487.
11. Ramaswami M, Taylor JP, Parker R. Altered ribostasis: RNA-protein granules in degenerative disorders. *Cell*. 2013;154:727–736.
12. Dreyfuss G, Matunis MJ, Pinol-Roma S, Burd CG. hnRNP proteins and the biogenesis of mRNA. *Annu Rev Biochem*. 1993;62:289–321.
13. Mayeda A, Munroe SH, Caceres JF, Krainer AR. Function of conserved domains of hnRNP A1 and other hnRNP a/B proteins. *EMBO J*. 1994;13:5483–5495.
14. Guil S, Long JC, Caceres JF. hnRNP A1 relocalization to the stress granules reflects a role in the stress response. *Mol Cell Biol*. 2006;26:5744–5758.
15. Molliex A, Temirov J, Lee J, et al. Phase separation by low complexity domains promotes stress granule assembly and drives pathological fibrillization. *Cell*. 2015;163:123–133.
16. Munder MC, Midtvedt D, Franzmann T, et al. A pH-driven transition of the cytoplasm from a fluid- to a solid-like state promotes entry into dormancy. *Elife*. 2016;5:e09347.
17. Li YR, King OD, Shorter J, Gitler AD. Stress granules as crucibles of ALS pathogenesis. *J Cell Biol*. 2013;201:361–372.
18. Liu Q, Shu S, Wang RR, et al. Whole-exome sequencing identifies a missense mutation in hnRNPA1 in a family with flail arm ALS. *Neurology*. 2016;87:1763–1769.
19. Purice MD, Taylor JP. Linking hnRNP function to ALS and FTD pathology. *Front Neurosci*. 2018;12:326.
20. Baradaran-Heravi Y, Van Broeckhoven C, van der Zee J. Stress granule mediated protein aggregation and underlying gene defects in the FTD-ALS spectrum. *Neurobiol Dis*. 2020;134:104639.

21. Das RK, Pappu RV. Conformations of intrinsically disordered proteins are influenced by linear sequence distributions of oppositely charged residues. *Proc Natl Acad Sci U S A*. 2013; 110:13392–13397.
22. Chong PA, Vernon RM, Forman-Kay JD. RGG/RG motif regions in RNA binding and phase separation. *J Mol Biol*. 2018;430:4650–4665.
23. Patel SS, Belmont BJ, Sante JM, Rexach MF. Natively unfolded nucleoporins gate protein diffusion across the nuclear pore complex. *Cell*. 2007;129:83–96.
24. Kedersha N, Anderson P. Stress granules: Sites of mRNA triage that regulate mRNA stability and translatability. *Biochem Soc Trans*. 2002;30:963–969.
25. King OD, Gitler AD, Shorter J. The tip of the iceberg: RNA-binding proteins with prion-like domains in neurodegenerative disease. *Brain Res*. 2012;1462:61–80.
26. Choi KJ, Tsoi PS, Moosa MM, et al. A chemical chaperone decouples TDP-43 disordered domain phase separation from fibrillation. *Biochemistry*. 2018;57:6822–6826.
27. Ferreon JC, Jain A, Choi KJ, et al. Acetylation disfavors tau phase separation. *Int J Mol Sci*. 2018;19:1360.
28. Weber SC, Brangwynne CP. Getting RNA and protein in phase. *Cell*. 2012;149:1188–1191.
29. Pace CN, Fu H, Lee Fryar K, et al. Contribution of hydrogen bonds to protein stability. *Protein Sci*. 2014;23:652–661.
30. Ferreon AC, Deniz AA. Alpha-synuclein multistate folding thermodynamics: Implications for protein misfolding and aggregation. *Biochemistry*. 2007;46:4499–4509.
31. Babinchak WM, Haider R, Dumm BK, et al. The role of liquid-liquid phase separation in aggregation of the TDP-43 low-complexity domain. *J Biol Chem*. 2019;294:6306–6317.
32. Mompean M, Chakrabartty A, Buratti E, Laurents DV. Electrostatic repulsion governs TDP-43 C-terminal domain aggregation. *PLoS Biol*. 2016;14:e1002447.
33. Babinchak WM, Dumm BK, Venus S, et al. Small molecules as potent biphasic modulators of protein liquid-liquid phase separation. *Nat Commun*. 2020;11:5574.
34. Kamagata K, Kanbayashi S, Honda M, et al. Liquid-like droplet formation by tumor suppressor p53 induced by multivalent electrostatic interactions between two disordered domains. *Sci Rep*. 2020;10:580.
35. Martin EW, Thomasen FE, Milkovic NM, et al. Interplay of folded domains and the disordered low-complexity domain in mediating hnRNPA1 phase separation. *Nucleic Acids Res*. 2021;49:2931–2945.
36. Gui X, Luo F, Li Y, et al. Structural basis for reversible amyloids of hnRNPA1 elucidates their role in stress granule assembly. *Nat Commun*. 2019;10:2006.
37. Schindelin J, Arganda-Carreras I, Frise E, et al. Fiji: An open-source platform for biological-image analysis. *Nat Methods*. 2012;9:676–682.

How to cite this article: Tsoi PS, Quan MD, Choi K-J, Dao KM, Ferreon JC, Ferreon ACM. Electrostatic modulation of hnRNPA1 low-complexity domain liquid–liquid phase separation and aggregation. *Protein Science*. 2021;30:1408–1417. <https://doi.org/10.1002/pro.4108>